Confinement of a potassium plasma in a spindle cusp magnetic field

R. A. Bosch[a] and R. L. Merlino
Department of Physics and Astronomy, The University of Iowa, Iowa City, Iowa 52242

(Received 19 May 1986; accepted for publication 22 July 1986)

The confinement properties of a low-β (average) potassium plasma produced by contact ionization in a spindle cusp magnetic field were investigated. In this configuration, $n_e \approx 10^8$–10^{10} cm^{-3}, $T_e \approx T_i \approx 0.2$ eV, and the ions are weakly magnetized. Electron and ion densities, space potentials, and plasma flow velocities were measured in the ring and point cusps. The leak width of the escaping plasma was measured over a wide range of magnetic field strengths and neutral pressures. The dependence of the leak width on neutral pressure and magnetic field strength is accounted for by a simple model in which the plasma streams out of the cusps along the magnetic field lines while diffusing across the magnetic field due to the combined effects of neutral-particle collisions and Bohm diffusion. Measurements of broadband plasma noise suggest the presence of ion acoustic wave turbulence.

I. INTRODUCTION

Magnetic field geometries containing cusps are widely used in laboratory devices for basic plasma-physics studies, due to their ability to confine large-volume uniform quiescent plasmas.[1] In addition, magnetic cusps are being investigated for use in thermonuclear fusion plasma confinement schemes,[2–4] ion-beam sources,[5] and plasma-etching reactors.[6] The efficiency of such devices depends on plasma losses through the cusps.

Of particular interest are the profiles of plasma escaping through the cusps (characterized by their full width at half maximum (FWHM)—the so-called cusp leak width), the plasma flow velocity in the cusps, and the electrostatic potentials in the cusps. These properties have been examined quite extensively in low-β discharge devices,[2,4,7–9] and numerous interpretations have been given. The interpretations include considerations of electrostatic effects,[2,4,10] neutral-plasma collisions,[2,4,11] turbulence,[2,4,12] and the presence of high-energy primary electrons.[13]

We have recently conducted an investigation of the confinement of an argon discharge plasma in a magnetic spindle cusp,[14] in which we measured ion and electron densities, space potentials, and flow velocities in the ring and point cusps over a wide range of plasma density, neutral pressure, and magnetic field strength. Our results suggested that electrostatic fields inhibited the flow of ions across the magnetic field, in accordance with the findings of other experimenters.[8,9] The dependence of the leak width upon the magnetic field and neutral pressure was accounted for by a simple model in which the plasma streams out of the cusps at the ion acoustic speed while diffusing across the magnetic field due to the combined effects of neutral-particle collisions and Bohm diffusion.

Our results suggested that in typical discharge cusp experiments, diffusion of particles due to Bohm diffusion and neutral-plasma collisions are of comparable magnitude, and the relative importance of these processes depends upon the magnetic field strength and neutral pressure. Since the magnetic field strength varies in a cusp geometry, one could even have the more complex situation where Bohm diffusion is the dominant mode of cross-field particle transport in the regions of high magnetic field, while at the same time neutral-plasma collisions are responsible for most of the cross-field particle transport in the low-field regions. The ability to minimize the effects of neutral-plasma collisions is limited by the difficulty of maintaining a discharge at pressures below $\sim 10^{-5}$ Torr. Furthermore, such low-pressure discharges contain relatively high concentrations of primary electrons,[15] which may also affect the plasma dynamics and complicate the Langmuir probe measurements. At high neutral pressures, where Bohm diffusion is less important, the flow of plasma along magnetic field lines is also affected by collisions, adding a further complication. Finally, the volume production of plasma by primary electrons, which themselves have a characteristic leak width dependent upon their energy and the magnetic field strength, will presumably have some effect upon the leak widths.

By investigating the confinement of an alkali-metal plasma produced by contact ionization, we were able to essentially eliminate the effects of collisions and also to eliminate the effects of primary electrons and the resultant volume production of plasma. Potassium was chosen since its ion mass (39) is nearly the same as that of argon (40). The absence of primary electrons simplified the measurement of the plasma potential, since the floating potential of a cold probe was relatively close to the plasma potential.

In order to compare the behavior of the potassium plasma with that of the argon discharge previously studied, we performed many of the same measurements. The plasma density, potential profiles, and velocity of the escaping plasma were measured in both the ring and point cusps. The dependence of the electron and ion leak widths on plasma density was determined over a wide range of densities. At densities sufficiently high that the plasma was quasineutral, it was observed that the ion leak width was smaller than at lower densities, presumably due to self-consistent electric fields. This behavior was previously observed in the argon discharge plasma.[14] The leak width measurements were made over a large range of magnetic field strength so that the

[a] Present address: Nuclear Engineering Department, University of Michigan, Ann Arbor, MI 48109.

 0021-8979/86/213056-12$02.40

scaling could be determined. Neutral helium gas was added to the plasma in order to investigate the effects of plasma-neutral collisions; leak widths were then measured over a broad range of neutral gas pressure and magnetic field strength to determine the scaling laws in the presence of plasma-neutral collisions. As in the argon discharge, the observed scalings could be accounted for by a model in which plasma streams out of the cusps at the ion acoustic speed while diffusing across the magnetic field due to the combined effects of Bohm diffusion and neutral-plasma collisions.

In addition, we measured the spectrum of plasma oscillations in the ring cusp for different magnetic field strengths. The scaling of the prominent noise frequency with magnetic field strength suggests that part of the observed noise is due to ion acoustic waves.

The apparatus and experimental techniques are described in Sec. II. In Sec. III we present the experimental results, which are then discussed in Sec. IV. The results and conclusions are summarized in Sec. V.

II. EXPERIMENTAL APPARATUS

The experimental apparatus is shown in Fig. 1. A cylindrical stainless-steel chamber, 90 cm in length and 60 cm in diameter, was evacuated to a base pressure of $\sim 5\times 10^{-7}$ Torr. The chamber contained two water-cooled coils of 17 cm inner diameter, which produced a spindle cusp magnetic field using currents up to 1000 A. Each coil was made of six turns of 6.35-mm ($\frac{1}{4}$-in.) copper tubing in a Teflon insulating sleeve enclosed in an aluminum shell which was connected electrically to the grounded chamber. The maximum field produced in the center of the ring cusp was 160 G, while the maximum field in the center of the point cusp was 260 G.

An alkali-metal plasma was produced in the center of the chamber by contact ionization of potassium vapor on a hot tungsten foil, the same method of plasma production employed in Q machines.[16] In order to reduce the vapor pressure of the potassium, two cylindrical copper cold plates covered much of the inner surface of the chamber. The cold plates were cooled to ~ 5 °C by circulating a refrigerated solution of 39% propylene glycol in water through 6.35-mm ($\frac{1}{4}$-in.) copper tubing that was soldered to the cold plates. Further details of the apparatus have been described elsewhere.[17]

In order to avoid possible effects on the plasma behavior due to the voltage drop across the directly heated tungsten foil, the heating current to the tungsten foil was pulsed on and off at 60 Hz. This permitted measurements of the plasma during the heating off-cycle when there was no voltage drop across the foil. Typically, 70 A at 5 V were passed through the foil for $\frac{1}{120}$ s, followed by $\frac{1}{120}$ s during which no current was passed through the foil, producing an average heating power of 175 W.

The bias of the hot foil (with respect to the grounded chamber) affected the plasma production. When the foil was biased positively (>1 V), very little plasma was produced. When the foil was grounded or biased negatively (between 0 and -20 V), the resultant plasma density was fairly high (10^8–10^{10} cm^{-3}), the electron and ion density profiles depended little upon the bias voltage, and the plasma potential roughly followed the bias on the foil. In this case, a net electron current of a few milliamperes flowed through the plasma from the hot foil to the chamber walls, while for a positively biased foil a much smaller net ion current flowed from the hot foil to the chamber walls. The electron current flow increased when the foil was biased more negatively. The flow of this current through a layer of contaminants on the chamber wall surface may be responsible for the voltage drop between the chamber and the plasma, whose potential roughly followed the bias of the hot foil. The possibility that the voltage drop occurred in a plasma sheath appears to be less plausible since such a sheath would prevent ions from reaching the chamber walls and recombining when the plasma potential is very negative, in apparent contradiction with results (to be described later) indicating that the ions flowed from the hot foil, out of the cusps, to the chamber walls.

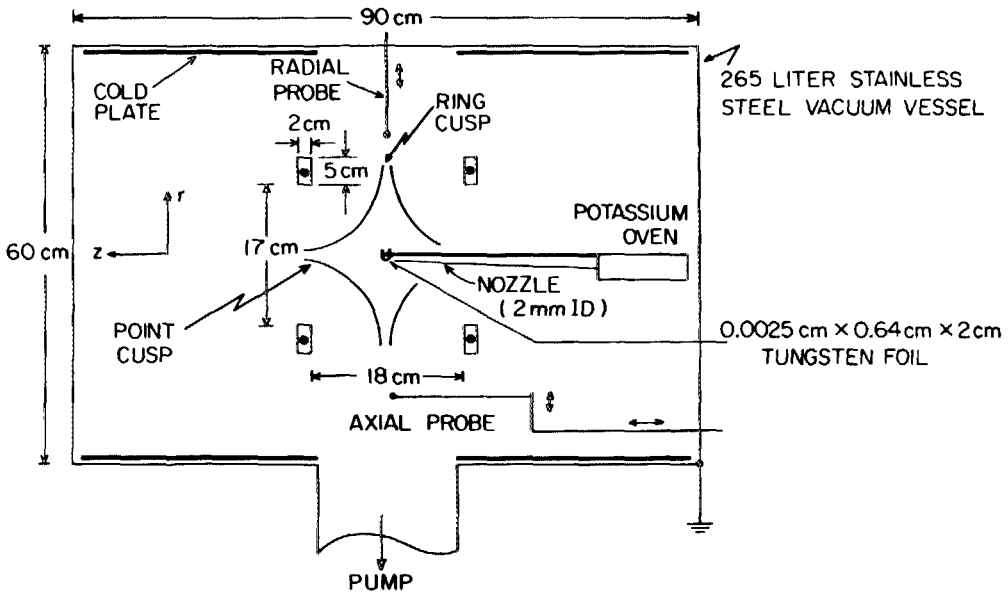

FIG. 1. Schematic diagram of the spindle cusp potassium plasma device.

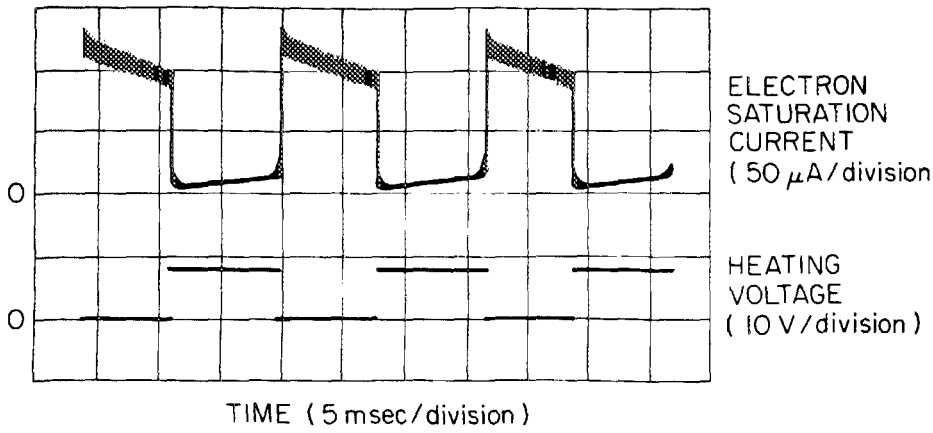

FIG. 2. Typical probe signal and tungsten foil-heating voltage signal.

We also studied the case when the foil was heated with a dc voltage of ~ 4 V. There was little difference between the plasma produced with a dc-heated foil and a pulse-heated foil, provided that the bias of the center of the foil (with respect to the grounded chamber) was the same in both cases.

In the remainder of our studies, one side of the tungsten foil was grounded, and the other side was pulsed with a positive voltage. Under these conditions very little plasma was created during the time when the foil was being heated, minimizing the possible influence of the foil-heating voltage on the measured plasma behavior. The resultant plasma density in the ring cusp (as measured by a Langmuir probe) as a function of time is shown in Fig. 2. When the heating cycle ended, the plasma density rose quickly (on a time scale of the ion transit time of $\sim 10^{-4}$ s). The plasma density then slowly decreased as the foil temperature dropped, leading to a 20% decrease in plasma density over $\frac{1}{120}$ s. Since this time scale is long compared with an ion-transit time, the plasma behavior during the heating off-cycle should be similar to that of a steady-state plasma. The typical densities were in the 10^8–10^{10} cm^{-3} range, comparable to densities in laboratory argon discharge devices. The electron and ion temperatures were ~ 0.2 eV, while the plasma noise level, determined from fluctuations in the electron- or ion-saturation currents drawn by a Langmuir probe and circuitry with a frequency response up to ~ 300 kHz, was $\delta n/n = 5$–15 %. We did not make any measurements of noise levels at higher frequencies ($\omega \sim \omega_{pe}$, the electron plasma frequency).

The plasma behavior was highly reproducible from one pulse to the next. As a result, the plasma properties at a given moment during the heating off-cycle were studied by using a sample and hold circuit triggered by a 60-Hz pulse with a width of ~ 0.1 ms. The part of the off-cycle that was sampled could be varied; little change of behavior (except for the gradual decay of plasma density) was observed throughout the off-cycle.

The major diagnostic used in this investigation was the Langmuir probe, typically a tantalum disk of 1.5 or 3 mm diam. Because of the limited spatial variation of the plasma potential (~ -4 to -2 V) and electron temperature, the relative ion density (as a function of position) was deter-

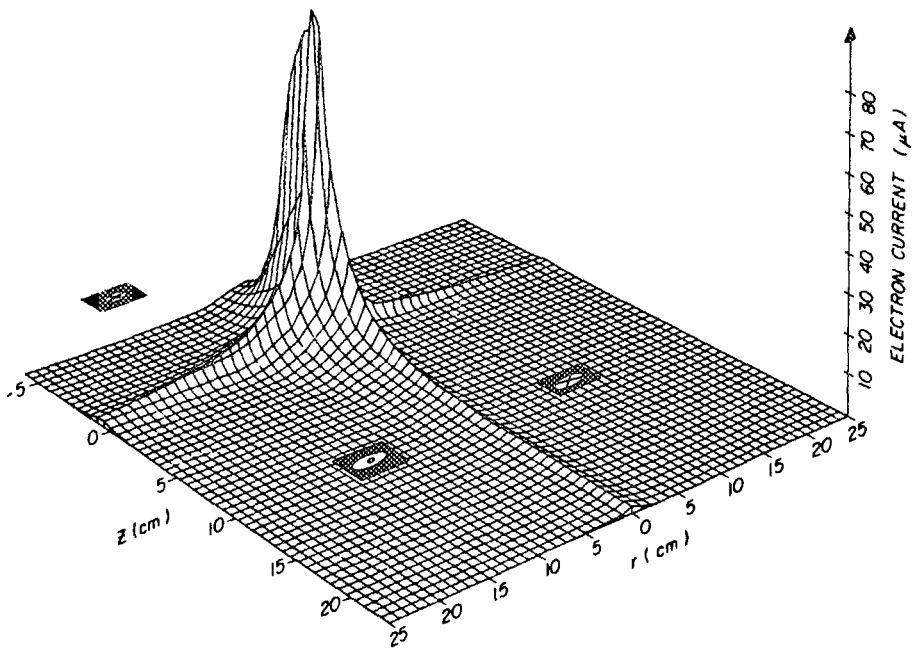

FIG. 3. Three-dimensional plot of the electron-saturation current drawn by a 1.5-mm disk Langmuir probe as it was moved through the vertical plane containing the axis. The distance from the axis is r, while z is the directed distance from the midplane. This plot was taken with a magnetic field of 130 G in the center of the ring cusp and 210 G in the center of the point cusp.

mined by measuring the probe current with the probe biased at -9 V, while the electron density was determined with the probe biased at 0 or $+9$ V. By observing the plasma properties with one probe while changing the bias on another probe, we determined that the probes did not significantly perturb the plasma.

III. EXPERIMENTAL RESULTS

We begin the presentation of the experimental results by showing, in Fig. 3, an overall three-dimensional perspective view of the relative electron density (i.e., electron saturation current) throughout the cusp. A similar plot for ions was also obtained. The density was largest near the hot foil, where the electrons and ions are produced. The escape of plasma through the ring and point cusps is evident, as is the confinement of plasma to a neighborhood of the axis and the midplane (the symmetry plane midway between the coils). The plasma displays a high degree of symmetry with respect to rotations about the axis, in spite of the lack of azimuthal symmetry in the hot-foil geometry. This may reflect the relative ease of cross-field plasma flow in the low magnetic field region near the hot foil as well as the presence of azimuthal particle drifts ($\mathbf{E}\times\mathbf{B}$ and $\nabla n\times\mathbf{B}$) which tend to equalize the density.

In comparison with the profiles obtained in an argon discharge spindle cusp,[14] the plasma density on the axis drops more rapidly as one moves away from the center of the device. This difference in behavior apparently results from the fact that the potassium plasma is produced only on the

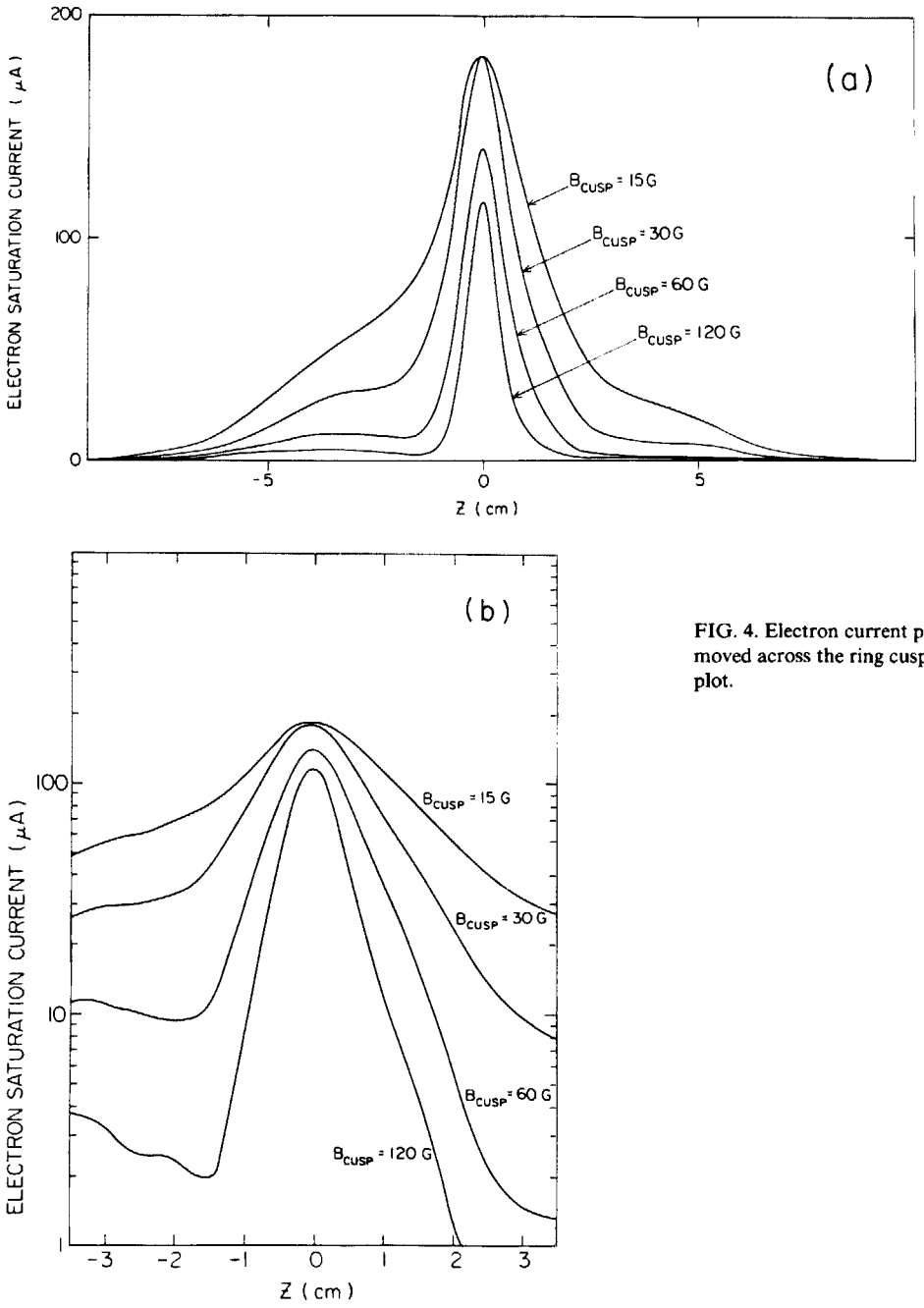

FIG. 4. Electron current profiles taken with a 3-mm disk Langmuir probe moved across the ring cusp at $r = 14$ cm. (a) Linear plot and (b) semilog plot.

hot foil, while volume production of argon plasma occurs throughout the regions populated by primary electrons. In this sense, the potassium plasma is similar to laser-produced plasmas in cusps[18] in that the plasma expands from the center.

In Fig. 4(a), we present typical profiles of the electron saturation current drawn by a Langmuir probe as it was moved across the ring cusp. The ion profiles were similar. As the magnetic field was increased (by increasing the coil current), the plasma profile became narrower. The profiles are plotted on a semilogarithmic scale in Fig. 4(b), showing that the narrow profiles observed with large magnetic field strengths adhere closely to the shape $n(z) = n_0 \exp(-2|z|/d)$, except in the immediate vicinity of the midplane. The presence of the foil support and nozzle (on the left-hand side in this figure) apparently caused a slight lack of symmetry with respect to reflections in the midplane ($z \rightarrow -z$); however, the surface area of the foil support protruding into the plasma was much less than the loss area at the spindle and point cusps.

A. Quasineutrality

As in the previously studied argon discharge spindle cusp,[14] similar electron and ion profiles could only be attained at sufficiently high density. The dependence of electron and ion leak widths upon density (via the dimensionless parameter $\omega_{pe}/\omega_{ce} \propto \sqrt{n_e}$, where ω_{pe}/ω_{ce} is the ratio of the electron plasma frequency to the electron gyrofrequency in the center of the cusp) is shown in Fig. 5. The density was varied by changing the temperature of the hot foil while holding all other parameters constant. For $\omega_{pe}/\omega_{ce} < 0.2$, the electron and ion leak widths were very different and the ion leak width was on the order of the ion gyrodiameter (5.2 cm), while for $\omega_{pe}/\omega_{ce} > 0.5$ the ion and electron profiles are similar, consistent with quasineutrality. For $\omega_{pe}/\omega_{ce} < 0.1$, the measured electron leak width was nearly equal to the probe diameter; thus the actual electron leak width may be smaller than measured. At sufficiently high densities ($\omega_{pe}/\omega_{ce} > 0.5$), the ion leak width was smaller than that at lower densities, suggesting that self-consistent electric fields reduce the cross-field ion transport. For the quasineutral case, the electron and ion leak widths depended only slightly upon the density ($d \propto n^{0.2}$). The remainder of our investigations describe the case in which the density was sufficiently high to ensure quasineutrality.

B. Leak widths

The scaling of the ring cusp leak width (FWHM), d, with magnetic field is shown in Fig. 6. [In Figs. 6–8, and 12(b), m denotes the slope of the line.] The observed dependence $d \propto B^{-1/2}$ is not consistent with any gyroradii ($d \propto B^{-1}$) and is the same scaling observed previously in an argon discharge spindle cusp[14] at the lowest pressures investigated, when the effect of plasma-neutral collisions was reduced.

To investigate the effects of collisions on the leak width, neutral helium was introduced into the vacuum chamber. The helium was not ionized and increased the rate of plasma-neutral collisions. The scaling of the ring cusp leak widths with neutral pressure, for two different magnetic field strengths, is shown in Fig. 7. For sufficiently high pressures, the leak width was broadened and scaled approximately as $d \propto P^{1/2}$. For the lower magnetic field strength, the leak width became comparable to the coil separation at high pressures, and the plasma was apparently constrained mechanically by the coils.

The scaling of the ring cusp leak width with the magnetic field strength for various neutral pressures is shown in Fig. 8. At sufficiently high pressures and low magnetic field, the scaling $d \propto B^{-1}$ was approximately obeyed. The observed scaling $d \propto P^{1/2}B^{-1}$ for a plasma experiencing plasma-neutral collisions is identical to the scaling observed previously in an argon discharge spindle cusp.[14]

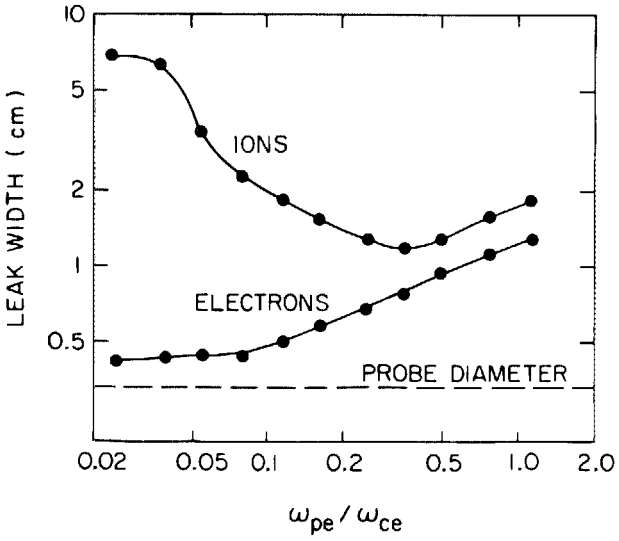

FIG. 5. Leak widths (full width at half maximum) of electron and ion profiles in the ring cusp vs ω_{pe}/ω_{ce}, with a magnetic field of 110 G in the center of the ring cusp. The plasma density was varied by changing the hot-foil temperature.

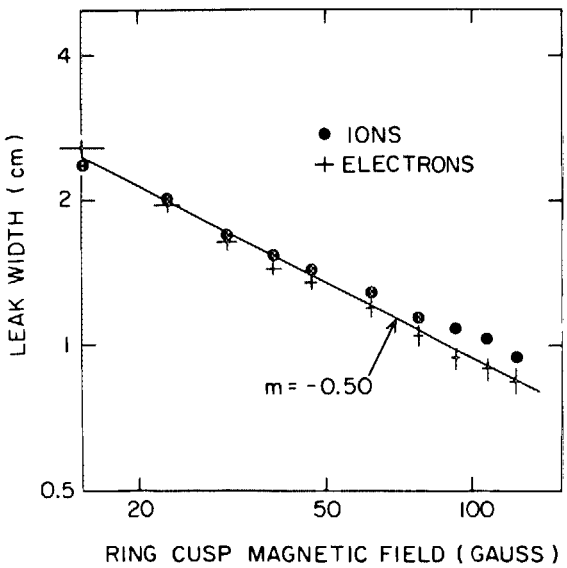

FIG. 6. Electron and ion leak widths in the ring cusp vs magnetic field strength. (In this and the following figures, m denotes the slope of the line.)

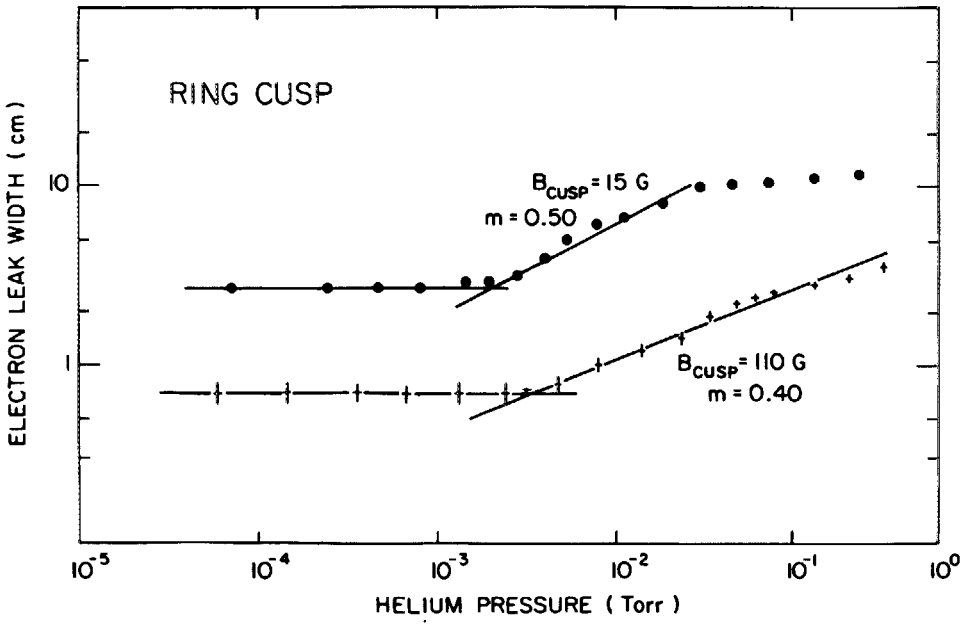

FIG. 7. Electron leak widths in the ring cusp vs neutral helium pressure for two different values of the magnetic field strength.

The electron and ion profiles in the point cusp were qualitatively similar to those in the ring cusp and had comparable leak widths to the ring cusp profiles. The dependence of the point cusp leak widths upon magnetic field and neutral helium pressure was also studied. As in the ring cusp, the scaling $d \propto B^{-1/2}$ was observed in the absence of helium while the scaling $d \propto P^{1/2}B^{-1}$ was approximately obeyed at sufficiently high pressures and low magnetic fields.[17]

C. Electrostatic potentials

The observed Langmuir traces indicated that the floating potential of a cold Langmuir probe is ~0.7 V lower than the plasma space potential. Thus the floating potential of a cold probe provided, up to a small voltage offset (~ -0.7 V), an accurate indication of the plasma potential. Measurements of the potential structures using the floating potential of a hot emissive probe agreed (up to an offset voltage of ~1–2 V, which increased with emissive probe temperature) with those measured using the cold-probe floating potential. This provided further confidence in the accuracy of using the cold-probe floating potential to measure the plasma space potential.

A three-dimensional overall perspective view of the cold-probe floating potential throughout the cusp is shown in Fig. 9. The potential structures were qualitatively similar to those measured previously in an argon discharge spindle cusp[14] and argon discharge line cusps,[8,9] with potential troughs providing cross-field confinement of ions. The potential of the bottom of the troughs was several tenths of a volt lower outside of the coils than in the center of the device, consistent with an acceleration of ions to their acoustic velocity as they flowed out of the cusp. The cross-field, ion-confining potential structure and the potential variation of the bottom of the point cusp trough are shown in Fig. 10. The ring cusp potential trough was similar.[17]

The average electric field strength in the trough was determined by dividing the depth of the trough by its width (full width at half maximum). The electric field strength was calculated in this way for a wide range of neutral pressure and magnetic field, as well as for the case when no helium was present. In all cases, the electric field strength agreed within a factor of 2 with the value $4kT_e/ed$, where d was the leak width measured under the same conditions.

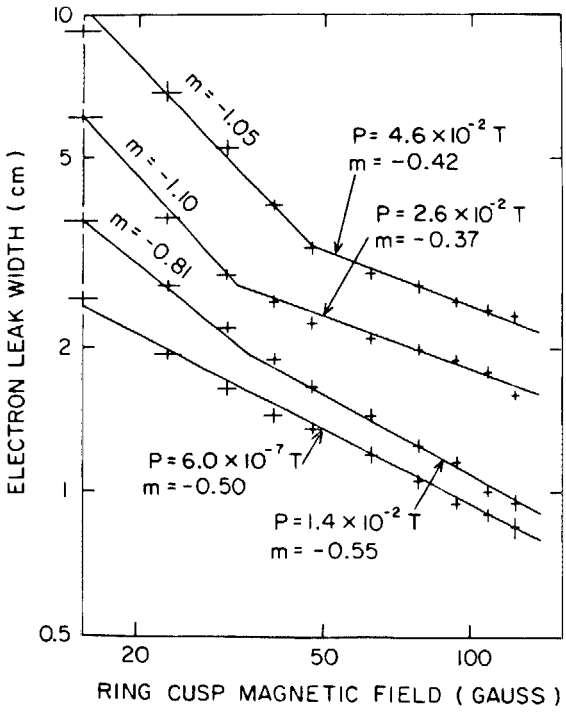

FIG. 8. Electron leak widths in the ring cusp vs magnetic field strength for different values of neutral helium pressure.

D. Flow velocities

The plasma flow velocities in the ring and point cusps were inferred from measurements of the propagation velocity of ion acoustic waves. The propagation velocity of ion acoustic waves in a plasma in which the ions are drifting is shifted by the ion-flow velocity. By subtracting the ion

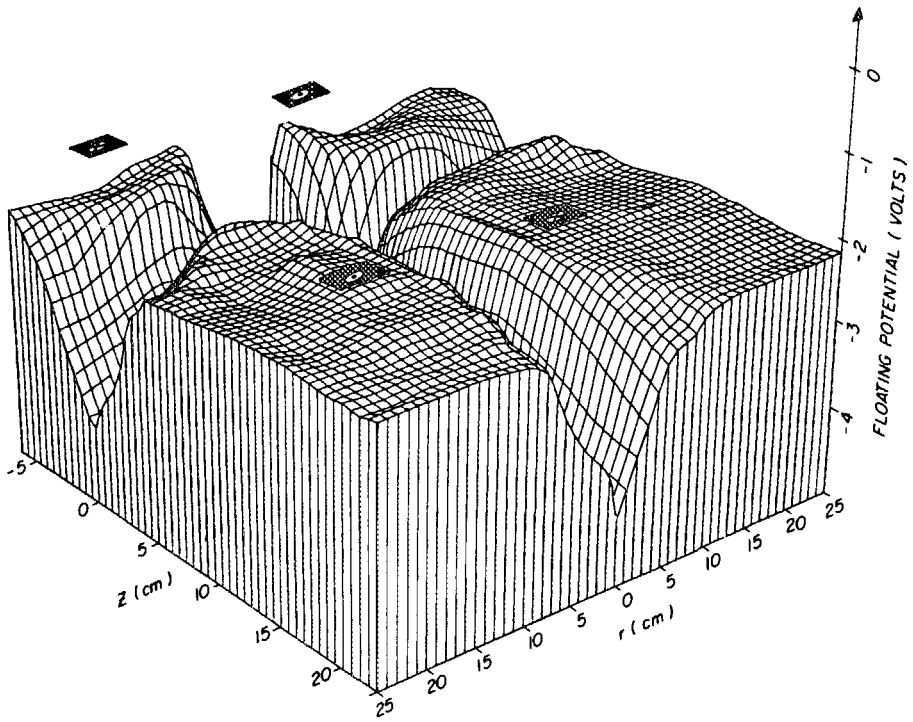

FIG. 9. Three-dimensional plot of the floating potential of a 1.5-mm disk Langmuir probe as it was moved through the vertical plane containing the axis. This plot was taken with a magnetic field of 130 G in the center of the ring cusp and 210 G in the center of the point cusp.

acoustic velocity C_s from the propagation velocity of ion acoustic waves, the flow velocity can be determined. All flow velocity measurements were made when no neutral helium gas was present.

Ion acoustic waves were launched into the point cusp using a circular launching grid of 5 cm diameter and 1×1-mm^2 mesh, which was placed between the hot tungsten foil and the point cusp at a distance of 3 cm from the center of the tungsten foil. The disturbance launched from the grid was detected by observing the ion current to a collecting probe in the point cusp.

When a single pulse was coupled to the grid, the leading

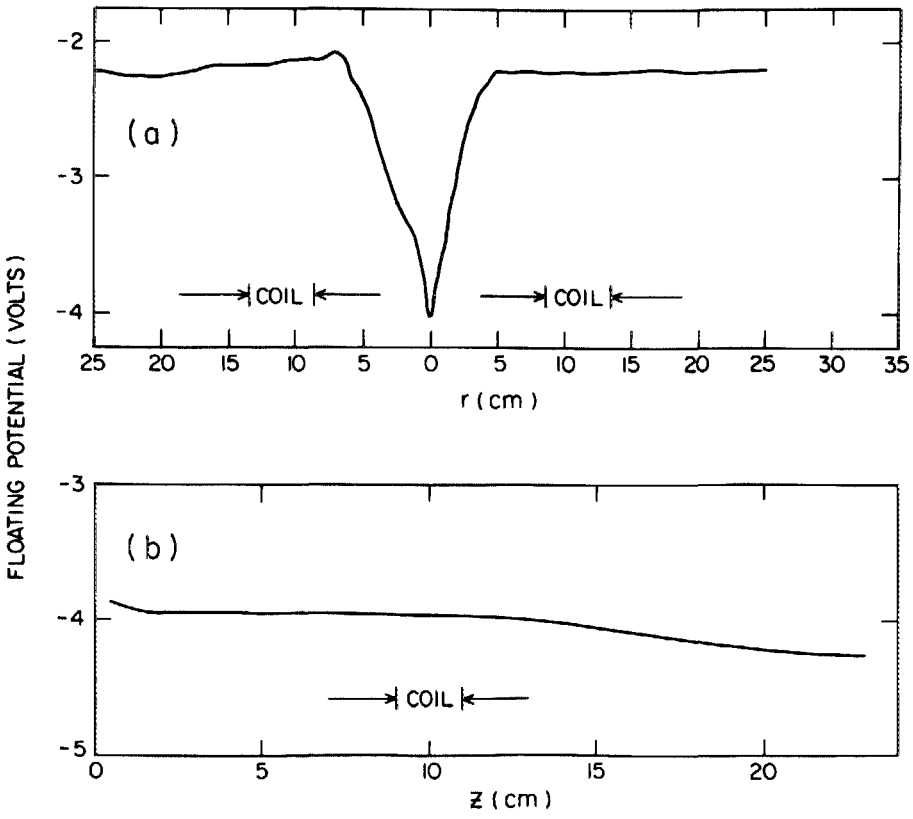

FIG. 10. Floating potential measurements in the point cusp. (a) Floating potential of a 1.5-mm disk Langmuir probe moved across the point cusp (at $z = 12$ cm) with a magnetic field of 210 G in the center of the point cusp. (b) Floating potential of a 1.5-mm disk Langmuir probe moved on axis in the point cusp under the same conditions.

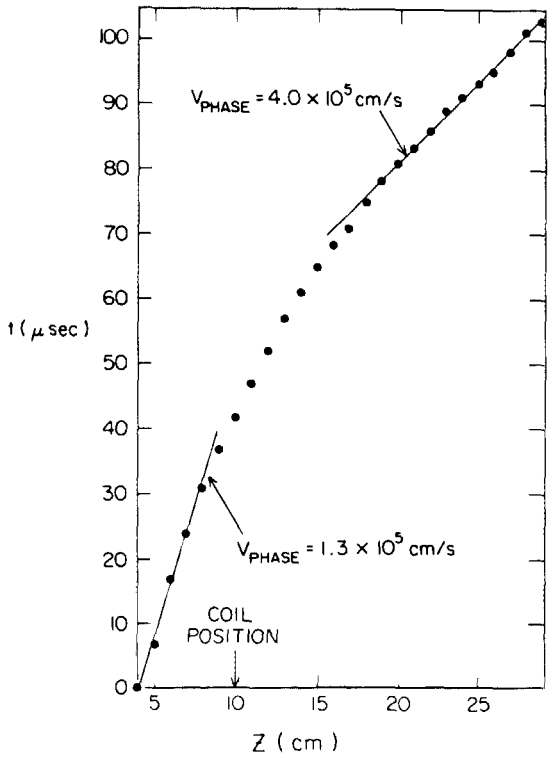

FIG. 11. Time of arrival of ion acoustic waves launched into the point cusp with a magnetic field of 210 G in the center of the point cusp.

edge of the resultant plasma disturbance was broadened, presumably due to enhanced Landau damping of the shorter wavelengths. This made it impossible to accurately measure the arrival time of the pulse at the probe. In order to circumvent this problem, a 1-V peak-to-peak 8-kHz sine wave was applied to the grid, which had a dc bias of -1.5 V. The time of arrival of the peaks of the traveling sine wave were then determined. The frequency of 8 kHz was chosen because it was sufficiently high to allow an accurate determination of the propagation time, yet it was sufficiently low so that the probe signal due to the ion acoustic wave greatly exceeded the direct coupling of the grid to the probe. The density perturbation due to the wave was $\delta n/n \approx 3\%$; a filter was used to improve the signal-to-noise ratio.

In Fig. 11, we display typical data showing the time of arrival of these waves versus probe position in the point cusp. The increase in the propagation velocity of the waves is not due to an increase in T_e, which was nearly constant throughout the device. Since the ion acoustic velocity $C_s = [k(T_e + 3T_i)/m_i]^{1/2} = (1.4 \pm 0.2) \times 10^5$ cm/s for $T_e = T_i = 0.2 \pm 0.05$ eV, these data show the acceleration in ion flow parallel to the magnetic field from a velocity of $\sim 0\, C_s$ to $\sim 1.8\, C_s$.

A similar investigation was carried out in the ring cusp, using a cylindrical grid 8 cm in diameter, 4 cm in length with a 3×3 mm^2 mesh. The grid was placed around the hot foil midway between the coils in an axially symmetric arrangement. The data show an acceleration in the ion flow from a velocity ~ 0.6 to $\sim 1.3\, C_s$ as the ions flow out of the ring cusps.[17] The acceleration of ions to supersonic velocities as they flow through the cusps was observed previously in an argon discharge spindle cusp.[14]

The conclusion that the ions flowed out of the cusps at the ion acoustic velocity is further supported by observations of the cusp plasma density versus time as the foil voltage is pulsed off and on (see, e.g., Fig. 2). These observations indicate that a time of 0.2 ms was required for the plasma density to build up or decay when the foil voltage was pulsed off or on. This indicates that plasma escaped with an average velocity on the order of $R/0.2$ ms $= 0.35\, C_s$ (where R is the coil radius), which is consistent with the acceleration of ions up to a speed of $\sim C_s$ as they flowed out of the cusps.

Measurements of the time of arrival of the wave peaks were taken at various positions throughout the ring and point cusps in order to determine the contours of constant phase.[17] In the ring cusp, the contours of constant phase coincided to a large degree with the surfaces of constant r, consistent with outwardly propagating cylindrical waves. In the point cusp, the contours of constant phase nearly coincided with the surfaces of constant z, consistent with axially propagating plane waves.

If there was a significant shear in the component of ion-flow velocity parallel to the magnetic field, one would expect ion acoustic waves to propagate faster along the field lines where the ion-flow velocity was greatest. The propagation of ion acoustic waves as cylindrical waves in the ring cusp and plane waves in the point cusp suggests that there is little shear in the component of ion-flow velocity along the magnetic field. However, the $\mathbf{E} \times \mathbf{B}$ and $\nabla n \times \mathbf{B}$ drift velocities vary throughout the cusp, so a significant shear in the azimuthal component of the electron-flow velocity might be expected. Since the electric field and plasma density gradient vary greatly over an ion gyrodiameter, the azimuthal ion velocities cannot be as easily estimated by consideration of these drifts.

In a plasma produced by contact ionization, the number of electrons and ions flowing from the hot foil into the plasma need not be equal. Typically, we measured several milliamperes of current flowing from the chamber walls to the hot foil during the time period when the foil was grounded. We can express this current as $I = en(v_{e\|} - v_{i\|})A$, where A is the plasma loss area at the cusp (e.g., $A = 2\pi Rd$ for the ring cusp) and $v_{e\|}$ and $v_{i\|}$ are electron and ion drifts parallel to B. Setting $v_{i\|} = C_s$, we estimate the parallel component of electron drift velocity out of the cusp to be on the order of a few times C_s. This is on the order of the azimuthal $\nabla n \times \mathbf{B}$ and $\mathbf{E} \times \mathbf{B}$ electron drifts expected in the cusps.

E. Plasma turbulence

The noise present throughout the potassium plasma (without helium) was studied by observing the fluctuations in electron current drawn by a probe, biased at $+9$ V, which were interpreted as the result of fluctuations in the electron density. Nearly identical fluctuations were observed when the probe was biased to collect ion current and when the floating potential was measured. This suggests that the turbulence was electrostatic and was not excited by the probe itself. The noise level was observed throughout the spindle cusp for the full range of magnetic field strengths studied. In

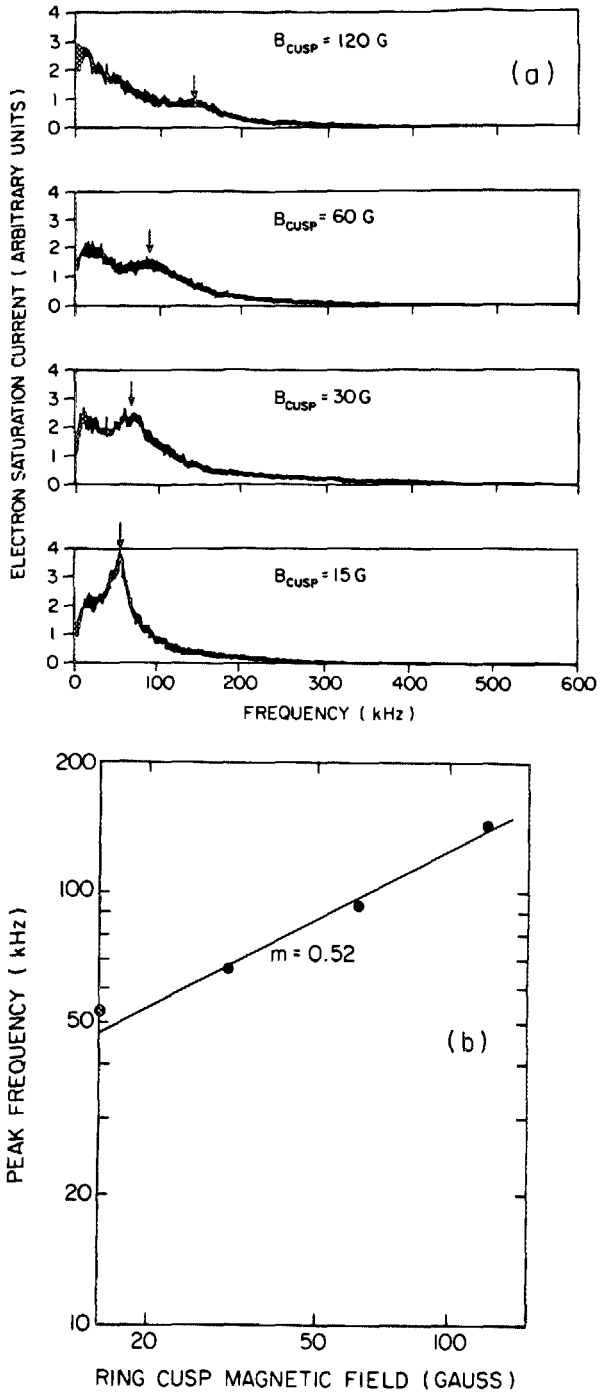

FIG. 12. Plasma noise measurements. (a) Spectra of electron-current fluctuations drawn by a 3-mm disk Langmuir probe in the center of the ring cusp for different values of the magnetic field. (b) Frequency of the peak in the electron-current fluctuation spectra of (a) vs magnetic field strength.

all cases we observed a relative fluctuation level $\delta n/n$ between 5% and 15%, using a probe and circuitry with a frequency response up to 300 kHz. Similar noise levels and frequencies were also observed when no magnetic field was present, and when the device was operated in a nonpulsed mode in which one side of the foil was biased negatively. We did not make any measurements of noise levels in the electron plasma frequency range.

For a probe located in the middle of the ring cusp, the observed fluctuation level $\delta n/n$ decreased from $\sim 15\%$ to $\sim 7\%$ as the magnetic field strength was increased from 15 to 150 G. This may be primarily due to an upward shift in the frequency of the noise, resulting in increased attenuation of the signal in the circuitry. For a given magnetic field strength, the absolute fluctuation level δn was greatest where the plasma density was greatest, while the relative fluctuation level $\delta n/n$ was greatest where n was least. (For example, $\delta n/n = 5\%$ near the hot foil, $\delta n/n = 10\%$ in the middle of the ring cusp, and $\delta n/n = 15\%$ in the ring cusp several centimeters from the midplane.)

The spectrum of electron current fluctuations drawn by a probe in the center of the ring cusp, using circuitry with a frequency response up to 100 kHz, is shown in Fig. 12(a) for four magnetic field strengths. Similar spectra were observed when the device was operated in a nonpulsed mode with one end of the hot foil biased negatively and one end grounded. The frequency range of this noise far exceeds the ion-cyclotron frequency ($f_{ci} < 10$ kHz in all cases), and corresponds to the frequencies expected from ion acoustic waves with wavelengths on the order of the plasma dimensions. A spectrum taken in the nonpulsed mode with no magnetic field present had a maximum amplitude at 8 kHz, the frequency expected for an ion acoustic wave whose wavelength equals the coil separation. The frequency of the local maximum in the noise spectrum [denoted by arrows in Fig. 12(a)] is plotted in Fig. 12(b). The frequency of this feature increases approximately as $B^{1/2}$.

IV. DISCUSSION AND INTERPRETATION OF RESULTS

A. Quasineutrality

At low plasma densities, the effects of plasma-generated electrostatic fields in the cusps will be negligible, so that the ion leak widths may be much larger than the electron leak widths. However, at sufficiently high densities quasineutrality must be attained, resulting in similar electron and ion leak widths. Our results, as well as previous discharge experiments[7,14] and a numerical study,[19] indicate that quasineutrality is attained largely through the cross-field electrostatic confinement of ions.

Our earlier results in an argon discharge spindle cusp,[14] as well as the numerical studies by Clark,[19] agree with a model in which the transition to quasineutrality occurs when

$$d/\lambda_{De} = \sqrt{10 T_i/T_e}\,, \tag{1}$$

where d is the electron leak width in the cusp and λ_{De} is the electron Debye length in the center of the cusp.[14] In the case where $T_e = T_i$, this corresponds to the standard criterion that the Debye length must be smaller than the plasma density scale length in order to have quasineutrality. Writing $d/\lambda_{De} = (d/r_{ce})(r_{ce}/\lambda_{De})$ and noting that $r_{ce}/\lambda_{De} = \omega_{pe}/\omega_{ce}$, we can rewrite Eq. (1) as

$$\omega_{pe}/\omega_{ce} = (r_{ce}/d)\sqrt{10 T_i/T_e}\,. \tag{2}$$

For the conditions illustrated in Fig. 5, $T_e = T_i = 0.2$ eV, $B = 110$ G, and $r_{ce} = 0.01$ cm, so that $d/r_{ce} = 50$. Equation (2) then predicts the transition to quasineutrality will occur when $\omega_{pe}/\omega_{ce} = 0.06$, in qualitative agreement with

the data. Thus, Fig. 5 can be interpreted as the attainment of quasineutrality and cross-field confinement of ions due to electrostatic effects when $\lambda_{De} \ll d$.

B. Leak widths

The observed leak widths may be understood in terms of a model in which plasma escapes from the cusp at the ion acoustic speed while diffusing across the magnetic field.[2,14] In this model the leak width is

$$d = (2\bar{D}R/C_s)^{1/2}, \tag{3}$$

where $\bar{D}$ is the effective diffusion coefficient and R is the coil radius. In general, the diffusion coefficient will be determined by neutral-particle collisions (i.e., classical diffusion) and nonclassical diffusion (e.g., Bohm diffusion) and if we assume that these processes are linearly additive, we may write

$$D = D_c + D_B = \left(\frac{r_{ce}^2}{\tau_c}\right)\left(1 + \frac{T_i}{T_e}\right) + \frac{ckT_e}{16eB}, \tag{4}$$

where D_c and D_B are the classical and Bohm diffusion coefficients and τ_c is the electron-neutral collision time.[20] For the range of parameters investigated, diffusion due to Coulomb collisions is negligible compared to Bohm diffusion. At sufficiently low neutral pressures and high magnetic fields, Bohm diffusion dominates and Eq. (3) predicts a leak width

$$d = \left[\frac{2R}{C_s}\left(\frac{ckT_e}{16eB}\right)\right]^{1/2} \propto m_i^{1/4} T_e^{1/4} B^{-1/2} \tag{5}$$

for $T_e = T_i$. This expression agrees with the observed scaling with the magnetic field in the low neutral pressure, high magnetic field case, for which $D_B > D_c$ is expected. Numerically, the result of Eq. (5) (using $B = B_{\text{cusp}}/2$ as the "average" magnetic field in the cusp geometry) agrees within a factor of 2 with the observed leak widths. This is a reasonable agreement in light of the approximations used to obtain Eq. (3) and the uncertainty in the numerical factor ($\frac{1}{16}$) in the Bohm diffusion coefficient.

We remark also that the exponential shape of the narrow profiles observed with a large magnetic field [Fig. 4(b)] is expected under certain ideal circumstances when leak widths are due to diffusion.[14,17]

At sufficiently high neutral pressures and low magnetic fields, classical diffusion dominates and Eq. (3) predicts a leak width

$$d = \left[\frac{2R}{C_s}\left(\frac{r_{ce}^2}{\tau_c}\right)\left(1 + \frac{T_i}{T_e}\right)\right]^{1/2} \propto m_i^{1/4} (\sigma T_e)^{1/2} P^{1/2} B^{-1}, \tag{6}$$

for $T_i = T_e$, where σ is the electron-neutral collision cross section.

The scaling with pressure and magnetic field given by this expression agrees with the observed scaling for sufficiently high neutral pressure and low magnetic field. The dependence upon ion mass and magnetic field predicted by this equation has been previously observed in discharge plasmas.[7] The numerical value of the leak width calculated from Eq. (6) agrees within a factor of 2 with the observed leak widths, a reasonable agreement in light of the approximations used to obtain Eq. (3).

C. Electrostatic potentials

The electrostatic potential measurements indicated the formation of negative troughs in the cusps, aligned along the magnetic field. The potential in the troughs decreases in the direction of plasma flow. These observations are in agreement with the self-consistent potentials expected in order to maintain quasineutrality. The electric fields parallel to **B** prevent the rapid escape of electrons while those perpendicular to **B** provide cross-field confinement of ions.

Because of the high mobility of electrons along field lines, we may expect a Boltzmann distribution of electron density along a given field line (with the exception of sheath regions near the center of the device and the chamber walls). This implies that the plasma potential along a given field line must decrease in the direction of decreasing density, i.e., the direction of flow. The density data and potential data of the point cusp (Figs. 3 and 10), as well as the ring cusp data, show that the potential along the field line in the center of the cusp decreases in the direction of flow by about 1–2 T_e, while the density decreases by about a factor of 3–10, in agreement with the behavior of a Boltzmann electron distribution. This decrease in potential along field lines is also consistent with the observed acceleration of ions to the ion acoustic velocity as they flow through the cusp. The potential and density measurements in the region between the hot foil and the cusps are not in agreement with a Boltzmann distribution, however, since the potential variation is smaller than that expected for the large density variation.

The ions in the cusps are moving at the ion acoustic velocity and thus have a kinetic energy on the order of $2kT_e$ (for $T_e = T_i$). In order to confine these ions in a trough of width d, the potential must rise by about $2kT_e/e$ within a distance $d/2$ of the center of the trough, giving rise to a perpendicular electric field of order $4kT_e/ed$. The data of Figs. 9 and 10, as well as the data taken through a wide range of neutral pressures and magnetic field strengths, show that the perpendicular electric field strengths in all cases agree within a factor of 2 with this value.

Thus the observed electrostatic potentials are in reasonable qualitative and quantitative agreement with the self-consistent potentials expected in order to maintain quasineutrality, thus providing cross-field confinement of the ions.

D. Flow velocities

The density profiles (see, e.g., Fig. 3) show that the plasma leak width in the spindle and point cusps is smallest where the magnetic field is greatest, suggesting that the plasma flow converges inside of the magnet coils and diverges outside of the coils. In addition, the density decreases in the direction of plasma flow. Under these circumstances, we may expect the acceleration of ions to a supersonic velocity as they pass through the cusp as has been observed previously in our argon discharge experiments in the spindle cusp,[14] in a Q machine in a magnetic mirror configuration[21] and in a multidipole line cusp experiment.[22] The acceleration of ions to supersonic velocities is also expected based on our plasma potential measurements in the cusp [see Fig. 10(b)]. Our

measurements (Fig. 11) indeed show that supersonic flow is achieved in the cusp consistent with previous observations.

E. Plasma turbulence

The subject of instabilities in cusps and turbulent broadening of the leak width has been discussed frequently.[2,4,12,23] Our observations suggest that the leak width of the collisionless cusp is determined by Bohm diffusion. This conclusion is supported by the leak-width scaling measurements as well as numerical estimates of the leak width. The electrostatic cross-field confinement of ions suggests that the rate of cross-field *electron* diffusion is responsible for the observed leak widths. Bohm diffusion of electrons is usually attributed to excessive electron drifts due to random electric fields arising from turbulent plasma oscillations.[24] These electric fields could perhaps be caused by high-frequency noise ($\omega \sim \omega_{pe}$) such as that we observed earlier in an argon discharge spindle cusp,[25] or by the lower-frequency noise observed in both the argon discharge and potassium plasmas. The possibility that Bohm diffusion is due to such oscillations is supported by our observations of significant density fluctuations with $\delta n/n$ between 5% and 15%. If such is the case, plasma turbulence plays a dominant role in the cross-field transport of plasma in the collisionless cusp.

In an attempt to identify the waves responsible for the observed turbulence in the potassium plasma, we considered drift waves and electrostatic ion waves in the acoustic limit ($\omega \gg \omega_{ci}$). Wave modes that require magnetized ions appear to be inappropriate in our device, where the electric and magnetic fields change greatly within an ion gyrodiameter.

The spatial distribution of density fluctuations throughout the plasma is consistent with either drift wave or ion acoustic wave turbulence. The increase in $\delta n/n$ observed as the probe was moved into lower-density regions could be interpreted as an indication of drift wave production in the regions where the azimuthal drift velocities are expected to be largest, but this result can be interpreted equally well as the expected hydrodynamic growth of ion acoustic waves as they propagate into a region of lower density.

The expected frequency ranges of drift and ion acoustic waves, as well as their dependence upon the magnetic field, can be estimated on dimensional grounds. For example, when the ring cusp magnetic field strength is 120 G, the electron $\nabla n \times \mathbf{B}$ drift velocity is

$$v_{\nabla n \times \mathbf{B}} = \frac{kT_e}{eB}\frac{\nabla n}{n} = \frac{kT_e}{eB}\frac{2}{d} = 3.3\times 10^5 \text{ cm/s}$$

and the $\mathbf{E}\times\mathbf{B}$ drift velocity is in the same direction with

$$v_{\mathbf{E}\times\mathbf{B}} = (4kT_e/ed)(1/B) = 6.6\times 10^5 \text{ cm/s},$$

so that the electrons drift around the axis with a velocity $v_D \cong 10^6$ cm/s. Since ions are not well magnetized, their drift velocity cannot be easily estimated. We expect the maximum possible wavelength λ of drift waves to be determined by the azimuthal plasma dimensions (since $\omega = \mathbf{k}\cdot\mathbf{v}_D$). These vary between the circumference πd of the point cusp plasma (where $d \cong 1$ cm is the point cusp leak width) and the ring cusp circumference $2\pi R$ (where $R = 10$ cm is the coil radius). For drift waves with an aximuthal phase velocity $v_D = 10^6$ cm, these wavelengths correspond to frequencies (f) of 320 and 16 kHz, respectively ($f = v_D/\lambda$). A maximum possible frequency may be estimated by considering a wavelength equal to the Debye length. For a density of 10^9 cm^{-3}, the Debye length is 10^{-2} cm, which corresponds to a frequency of 100 MHz. Thus drift waves can be expected in the frequency range of 16 kHz to 100 MHz.

For ion acoustic waves, we expect the maximum wavelength to be determined by the plasma dimensions characterized by the leak width d (~ 1 cm) and the ring cusp circumference $2\pi R$ (~ 60 cm). For a phase velocity of $C_s = 1.4\times 10^5$ cm/s, these wavelengths correspond ($f = C_s/\lambda$) to frequencies of 140 and 2 kHz, while the frequency corresponding to the Debye length (10^{-2} cm) is 14 MHz. Thus ion acoustic waves can be expected in the range 2 kHz to 14 MHz. Most of the observed turbulence lies within both the drift wave and ion acoustic wave frequency ranges.

Similarly, we can estimate the dependence of the spectrum upon the magnetic field for the two types of waves. Since the leak width scales as $d \propto B^{-1/2}$, the drift velocities $v_{\nabla_{n\times\mathbf{B}}}$ and $v_{\mathbf{E}\times\mathbf{B}}$ scale as $B^{-1/2}$. Thus the total electron drift velocity v_D will also scale as $B^{-1/2}$. The ring cusp circumference and the Debye length are independent of B, so the corresponding frequencies ($f = v_D/\lambda$) scale as $B^{-1/2}$ due to the dependence of the drift velocity upon the magnetic field strength. For wavelengths determined by the circumference of the point cusp plasma, $\pi d \propto B^{-1/2}$, the corresponding frequency is independent of B; however, this frequency is about 320 kHz and nearly exceeds the observed frequency range. Thus for drift waves we expect that the decrease in drift velocities with increasing magnetic field will lead to a corresponding decrease in the noise-frequency range as B is increased.

For ion acoustic waves, the phase velocity C_s is independent of B. Since the ring cusp circumference and the Debye length are independent of B, the frequencies corresponding to these lengths are also independent of B. The leak width d scales as $B^{-1/2}$ in the absence of plasma-neutral collisions, so the frequency corresponding to this wavelength ($f = C_s/d$) scales as $B^{1/2}$. Therefore, for ion acoustic waves the decrease in plasma dimensions with increasing B suggests that the frequency of the spectrum will increase as B is increased.

The data of Fig. 12 show that the noise spectrum exhibits a peak which shifts toward higher frequencies as the magnetic field is increased. This frequency shift is expected for ion acoustic turbulence, but it is opposite to the effect expected for drift wave turbulence. The frequency of the peak in the spectrum approximately scales as $B^{1/2}$ and numerically is very close to the frequency C_s/d expected for ion acoustic waves with wavelengths determined by the cusp leak widths. The 8-kHz peak in the spectrum observed in the nonpulsed plasma with no magnetic field agrees closely with $C_s/2R$, the frequency expected for an ion acoustic wave with wavelength equal to the coil separation. Thus the observed dependence of the peak frequency upon magnetic field strength, as well as its numerical value with and without a magnetic field, suggests that the peak in the noise spectrum is due to ion-acoustic turbulence. However, much of the plasma noise is outside of this peak, so the possibility that drift waves also

contribute to the observed noise spectrum cannot be ruled out.

It is known that ion acoustic waves can be excited by particle drifts (e.g., the azimuthal $\mathbf{E}\times\mathbf{B}$ and $\nabla n\times\mathbf{B}$ drifts). The presence of electron drifts (on the order of a few times C_s) perpendicular to $\mathbf{B}$ in cusps has been inferred from measurements in argon discharge cusps.[9,26] However, the magnitude of the azimuthal electron drifts and electron drifts parallel to $\mathbf{B}$ in the potassium plasma was estimated earlier to be on the order of a few times C_s, far below the threshold for excitation expected theoretically when $T_e \approx T_i$.

V. SUMMARY AND CONCLUSIONS

Our major findings and conclusions may be summarized as follows:

(a) For $\omega_{pe}/\omega_{ce} > 0.5$ (i.e., $\lambda_{De} \ll d$), self-consistent electrostatic fields result in cross-field confinement of ions.

(b) For sufficiently high neutral pressures and low magnetic fields, the leak width scales as $P^{1/2}B^{-1}$, while at low neutral pressures and high magnetic fields it scales as $P^{0}B^{-1/2}$. These scalings are consistent with a model in which plasma diffuses across the field due to the combined effects of neutral-plasma collisions and noncollisional Bohm diffusion.

(c) The measured electrostatic potentials are in reasonable agreement with the self-consistent potentials expected to maintain quasineutrality, inhibiting the flow of electrons parallel to $\mathbf{B}$ and the flow of ions perpendicular to $\mathbf{B}$.

(d) Ions are accelerated to the ion acoustic velocity as they flow through the cusps.

(e) The level of plasma noise present in the plasma (5–15 %) appears sufficiently large to be a possible cause of Bohm diffusion. The frequency spectrum of the noise, and its dependence upon the magnetic field strength, suggest that part of the plasma noise may be due to ion acoustic waves.

ACKNOWLEDGMENTS

We wish to thank S. Cartier, N. D'Angelo, G. Knorr, and K. Clark for useful discussions, and A. Scheller for technical assistance. This work was supported in part by the Office of Naval Research (ONR) and by a Graduate College Block Grant from the University of Iowa.

[1] R. Limpaecher and K. R. MacKenzie, Rev. Sci. Instrum. **44**, 726 (1973).
[2] I. Spalding, in *Advances in Plasma Physics*, edited by A. Simon and W. B. Thompson (Interscience, New York, 1971), Vol. 4, p. 79.
[3] N. Hershkowitz and J. M. Dawson, Nucl. Fusion **16**, 4 (1976).
[4] M. G. Haines, Nucl. Fusion **17**, 811 (1977).
[5] K. N. Leung, R. D. Collier, L. B. Marshall, T. N. Gallaher, W. H. Ingham, R. E. Kribel, and G. R. Taylor, Rev. Sci. Instrum. **49**, 321 (1978).
[6] T. E. Wicker and T. D. Mantei, J. Appl. Phys. **57**, 1638 (1985).
[7] N. Hershkowitz, K. N. Leung, and T. Romesser, Phys. Rev. Lett. **35**, 277 (1975); K. N. Leung, N. Hershkowitz, and K. R. MacKenzie, Phys. Fluids **19**, 1045 (1976).
[8] S. Cartier, Master's thesis, Department of Physics and Astronomy, The University of Iowa, Iowa City, Iowa (1980); N. Hershkowitz, J. R. Smith, and J. R. DeKock, Plasma Phys. **21**, 823 (1979).
[9] N. Hershkowitz, J. R. Smith, and H. Kozima, Phys. Fluids **22**, 122 (1979).
[10] G. Knorr and D. Willis, Z. Naturforsch. **37a**, 780 (1982).
[11] C. Koch and G. Matthieussent, Phys. Fluids **26**, 545 (1983); I. S. Landman and F. R. Ulinich, Sov. J. Phys. **8**, 371 (1982).
[12] R. Jones, Nuovo Cimento **34**, 157 (1982); R. Yoshino and T. Sekiguchi, J. Phys. Soc. Jpn. **44**, 1694 (1978).
[13] G. Knorr and R. Merlino, Plasma Phys. Control. Fusion **26**, 433 (1984).
[14] R. A. Bosch and R. L. Merlino, Phys. Fluids **29**, 1998 (1986).
[15] N. Hershkowitz, J. R. DeKock, P. Coakley, and S. L. Cartier, Rev. Sci. Instrum. **51**, 64 (1980).
[16] R. W. Motley, *Q Machines* (Academic, New York, 1975).
[17] R. Bosch, Ph.D. thesis, Department of Physics and Astronomy, The University of Iowa, Iowa City, Iowa (1986).
[18] A. Kitsunezaki, M. Tanimoto, and T. Sekiguchi, Phys. Fluids **17**, 1895 (1974); S. Kogoshi, K. N. Sato, and T. Sekiguchi, J. Phys. D **11**, 1057 (1978); R. E. Pechacek, J. R. Grieg, M. Raleigh, D. W. Koopman, and A. W. DeSilva, Phys. Rev. Lett. **45**, 256 (1980); R. Yoshino, K. Sato, and T. Sekiguchi, J. Phys. Soc. Jpn. **50**, 2101 (1981).
[19] K. Clark, Master's thesis, Department of Physics and Astronomy, The University of Iowa, Iowa City, Iowa (1984).
[20] N. A. Krall and A. W. Trivelpiece, *Principles of Plasma Physics* (McGraw-Hill, New York, 1973).
[21] S. A. Andersen, V. O. Jensen, P. Nielsen, and N. D'Angelo, Phys. Fluids **12**, 557 (1969).
[22] K. N. Leung, R. E. Kribel, D. G. Fitzsimons, and G. R. Taylor, Phys. Lett. **60A**, 203 (1977).
[23] H. Kozima, K. Yamagiwa, and M. Kawaguchi, Phys. Lett. **106A**, 252 (1984); N. D'Angelo, H. L. Pécseli, and P. I. Petersen, Phys. Fluids **17**, 1853 (1974).
[24] F. F. Chen, *Introduction to Plasma Physics and Controlled Fusion*, Vol. 1 of *Plasma Physics* (Plenum, New York, 1984); L. Spitzer, Jr., Phys. Fluids **3**, 659 (1960).
[25] R. A. Bosch and R. L. Merlino, Beitr. Plasmaphys. **26**, 1 (1986); **26**, 13 (1986).
[26] T. Fujita, T. Ohnuma, and S. Adachi, Plasma Phys. **23**, 1019 (1981).